

Quantum phases of dimerized and frustrated Heisenberg spin chains with $s = 1/2, 1$ and $3/2$: an entanglement entropy and fidelity study

V. M. L. Durga Prasad Goli*

Solid State & Structural Chemistry Unit, Indian Institute of Science, Bangalore 560 012, India

Shaon Sahoo†

*Department of Physics, Indian Institute of Science,
Bangalore 560 012, India*

S. Ramasesha‡

*Solid State & Structural Chemistry Unit,
Indian Institute of Science, Bangalore 560 012, India*

Diptiman Sen§

Centre for High Energy Physics, Indian Institute of Science, Bangalore 560 012, India

We study here different regions in phase diagrams of the spin-1/2, spin-1 and spin-3/2 one dimensional antiferromagnetic Heisenberg systems with frustration (next-nearest-neighbor interaction J_2) and dimerization (δ). In particular, we analyze the behaviors of the bipartite entanglement entropy and fidelity at the gapless to gapped phase transitions and across the lines separating different phases in the $J_2 - \delta$ plane. All the calculations in this work are based on numerical exact diagonalizations of finite systems.

PACS numbers: 64.70.Tg, 75.10.Pq, 03.67.-a, 03.67.Mn

I. INTRODUCTION

Matter can appear in different quantum phases with exotic properties like charge density wave, magnetism, superconductivity, and so on. Studies of these phases and the transitions from one phase to the other are important and interesting for both academic and technological reasons. Two major tools from quantum information theory have been used extensively in recent years for studying the quantum phases of a system: quantum entanglement and fidelity. The idea of quantum entanglement originated in the study of quantum correlations of many-body systems^{1,2}. It is expected that even for moderately large system sizes, the entanglement entropy can identify the values of the parameters of the Hamiltonian where a quantum phase transition (QPT) occurs because the quantum correlations of the systems change significantly occurs when one goes across such a transition³. In recent years, entanglement entropy has been used to study quantum critical regions in various systems⁴⁻¹³. Quantum fidelity is a measure of how little the ground state of a system changes as one changes the parameters of the Hamiltonian. A large change in the fidelity is anticipated close to a QPT even if the system size is not very large¹⁴⁻²⁸.

In this paper, we study different quantum phases and quantum critical regions with frustration J_2 (next-nearest-neighbor coupling) and dimerization δ (an alternation in the nearest-neighbor couplings) of the spin-1/2, 1 and 3/2 Heisenberg antiferromagnetic systems in one

dimension by calculating the entanglement entropy and fidelity in the ground state of the system. In particular, we study the transition from a gapless to a gapped phase and the changes in the spin structure across different phase lines in the $J_2 - \delta$ plane for the spin-1/2, 1 and 3/2 systems. For the spin-1/2 and spin-1 systems, our numerical study contains the locations of different critical points and lines separating different phases in the phase diagrams which had been found earlier by other methods, such as the density matrix renormalization group method³⁵⁻⁴⁰. We compare our results with those reported previously (using different techniques) whenever possible. For the spin-3/2 system, we find that the entanglement entropy and fidelity helps us to estimate the locations of the various critical points and lines in the phase diagram.

There are some related works which we briefly mention here. The bipartite entanglement for the spin-1/2 $J_1 - J_2$ model (without dimerization) has been studied in different contexts, like the transition from the Neel to the spiral phase and the gapless to gapped phase transition along the J_2 -axis (see, for example,^{29,30}). The gapless to gapped phase transition has also been studied using the fidelity (as a function of J_2) of the first excited state with periodic boundary conditions³¹ and the fidelity susceptibility of the ground state³². The role of entanglement between distant sites has been studied for this model with frustration and dimerization³³. To the best of our knowledge, the phase diagram of the spin-1 and spin-3/2 $J_1 - J_2$ model (with or without dimerization) has not yet been studied using entanglement entropy and fidelity. In this

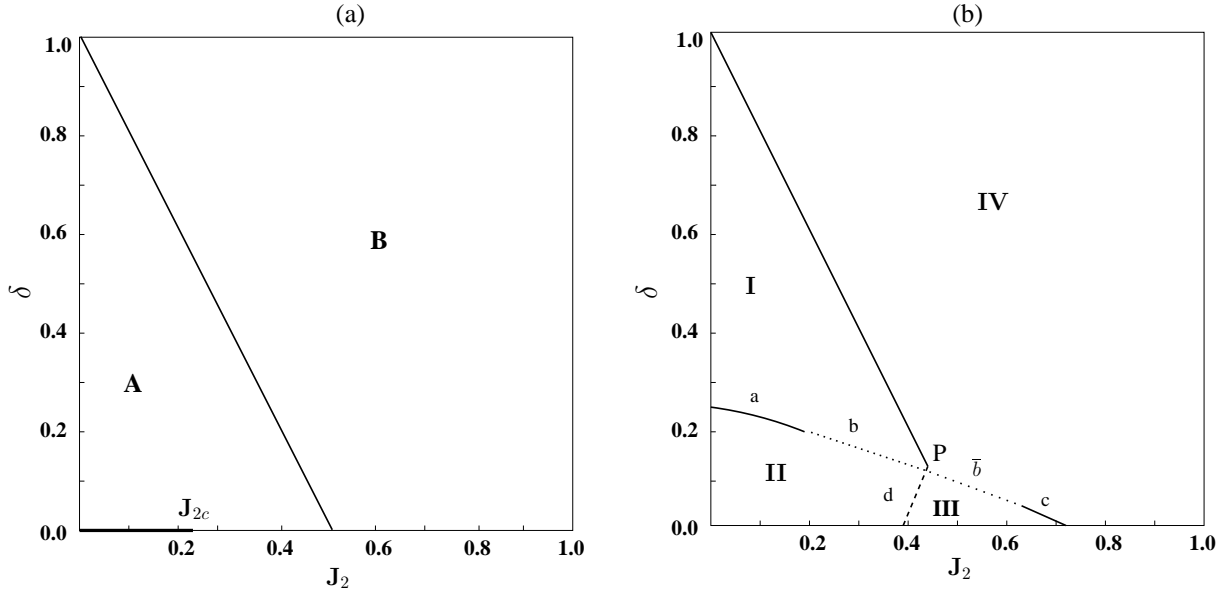


FIG. 1. Phase diagrams of the (a) spin-1/2 and (b) spin-1 chains in the $J_2 - \delta$ plane.

paper we report results on the entanglement entropy and fidelity of the $J_1 - J_2 - \delta$ model over the $J_2 - \delta$ plane.

Our paper is organized in the following way. In section II, we discuss how to calculate the entanglement entropy and fidelity. We then introduce the Hamiltonian that we study in section III. In section IV, we give a brief introduction to the numerical techniques we use in our work. We then present the entropy and fidelity results for the spin-1/2, spin-1 and spin-3/2 systems in section V. We conclude our paper in section VI.

II. ENTANGLEMENT ENTROPY AND FIDELITY

A pure state of a bipartite entangled system can be written as $|\psi\rangle = \sum_{ij} C_{ij} |\phi_i\rangle^l |\phi_j\rangle^r$, where $|\phi_i\rangle^l$ and $|\phi_j\rangle^r$ are the basis states of the left and right blocks respectively. The reduced density matrix (RDM) of the left block, $\rho_l = \text{Tr}_r(|\psi\rangle\langle\psi|)$, is calculated by tracing out the degrees of freedom of the right block. The elements of the RDM ρ_l are given by

$$\rho_{ij} = \sum_k C_{ik} C_{jk}^*. \quad (1)$$

The von Neumann entropy of a block is given by $S = -\text{Tr}(\rho \log_2 \rho)$ or

$$S = -\sum_i \lambda_i \log_2 \lambda_i, \quad (2)$$

where the λ_i 's are the eigenvalues of ρ .

Fidelity measures how little a particular wave function (for instance, the ground state) changes with the parameters of a model Hamiltonian. This is quantified by the overlap of the wave function at two different parameter values. If p is a parameter then the fidelity is given by

$$F = |\langle\Psi(p)|\Psi(p+\alpha)\rangle|, \quad (3)$$

where α is a small variation in p . In our case, both J_2 and δ are parameters with respect to which we have calculated fidelity and we have taken the change in the parameter to be 10^{-2} in the numerical calculations.

III. DESCRIPTION OF THE SPIN MODEL

We study the Heisenberg Hamiltonian for the antiferromagnetic chain with both nearest-neighbor and next-nearest-neighbor couplings and dimerization^{34,36}. We will use this Hamiltonian for the spin-1/2, spin-1 and spin-3/2 systems; it is given by

$$H = J_1 \sum_{i=1}^{2N-1} (1 - (-1)^i \delta) \vec{S}_i \cdot \vec{S}_{i+1} + J_2 \sum_{i=1}^{2N-2} \vec{S}_i \cdot \vec{S}_{i+2} \quad (4)$$

where J_1 is the nearest-neighbor interaction (we take $J_1=1$ for our study), δ ($0 \leq \delta \leq 1$) is the dimerization and J_2 ($0 \leq J_2 \leq 2$) is the next-nearest-neighbor interaction. In our entropy contour plot we have taken the range of J_2 from 0 to 2.

The phase diagrams of the spin-1/2 and spin-1 chains are different from each other in the $J_2 - \delta$ plane (see Fig. 1). The spin-1/2 system undergoes a QPT from a gapless phase to a gapped phase at $J_{2c} = 0.2411 \pm 0.0001$ without dimerization ($\delta = 0$)⁴¹, while the rest of the

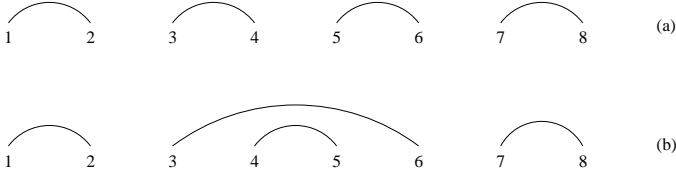


FIG. 2. Some legal valence bond diagrams of a spin-1/2 chain with 8 sites and total spin $S = 0$.

phase diagram is gapped. The line $2J_2 + \delta = 1$ separates the Neel phase (region A) from the spiral phase (region B)³⁶.

The spin-1 system has a number of distinct phases in the $J_2 - \delta$ plane. Region I denotes the spin Peierls gapped phase. Regions II and III are Haldane gapped and spiral regions respectively. In these two regions the ground state of an open chain is four-fold degenerate. Region IV is a spiral gapped phase with a non-degenerate ground state for an open chain. A gapless phase exists along the critical line ‘a’ that lies between $(0, 0.25)$ to $(0.22 \pm 0.02, 0.20 \pm 0.02)$ in the $J_2 - \delta$ plane^{38,39,42}. A line ‘c’ separating the regions II and III extends from $(0.73, 0)$ to $(0.65, 0.05)$; on that line the gap appears to be zero (to numerical accuracy). Along the dotted lines ‘b’ which extends from $(0.22 \pm 0.02, 0.20 \pm 0.02)$ to the point $P = (0.432, 0.136)$ and ‘b’ which extends from P to $(0.65, 0.05)$, the gap shows a minimum as a function of δ (see Fig. 12). This will be discussed more detail in section V.B.2. The line $2J_2 + \delta = 1$ starts at the point ‘P’ and extends up to $(0, 1)$, separating regions I and IV. Another line (‘d’) starts at $(0.39, 0)$ and ends at point ‘P’, separating regions II and III.

The phase diagram of spin-3/2 system has not been studied yet. We will show below that the entanglement entropy and fidelity of this system can give some insights into its phase diagram.

IV. NUMERICAL TECHNIQUES

For our calculations, we use the M_s basis (eigenstates of the z component of total spin)⁴³. These basis states are orthonormal and it is easy to obtain the RDM (which is used to calculate the entanglement entropy) when the states of the system are expressed in this basis. On the other hand, most of the results can be understood qualitatively using valence bond (VB) theory⁴⁴. In this theory^{45,46}, the basis states in the singlet space are expressed as products of pairwise singlets, which follow the Rumer-Pauling rules, to avoid overcompleteness of the VB states. Fig. 2 shows some VB-diagrams of a spin-1/2 chain with 8 sites and total spin $S = 0$. The VB state (a) is a Kekule state which is a product of nearest-neighbor singlets.

Since our Hamiltonian conserves total spin, all its eigenstates are also eigenstates of total spin. There-

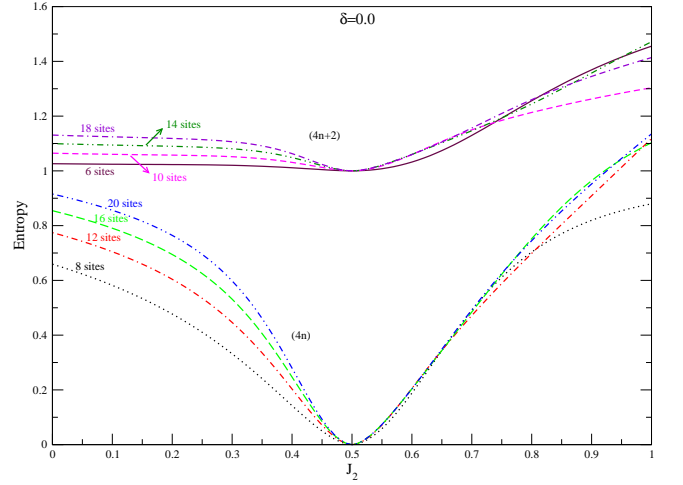


FIG. 3. Ground state entanglement entropy of the spin-1/2 system with different chain lengths at $\delta = 0$. The lower set of plots for $4n$ systems and the upper set of plots is for $4n+2$ systems.

fore, the eigenstates that we obtain by diagonalizing the Hamiltonian in the constant M_s basis will be linear combinations of the VB basis states. It may be worth mentioning here that appropriate linear combinations of constant M_s basis states can give different VB basis states⁴⁷. Now, a VB basis state contributes to the bipartite entanglement entropy of a state under study if the boundary between the two blocks of the system cuts a singlet line. If the boundary does not cut a singlet line, its contribution is assumed to be zero. For example, if the boundary goes through the sites 4 and 5 of the system, the entropy contribution of diagram (a) will be zero while that of diagram (b) will be non-zero (Fig. 2). Depending upon the entropy contributions of the VB basis states

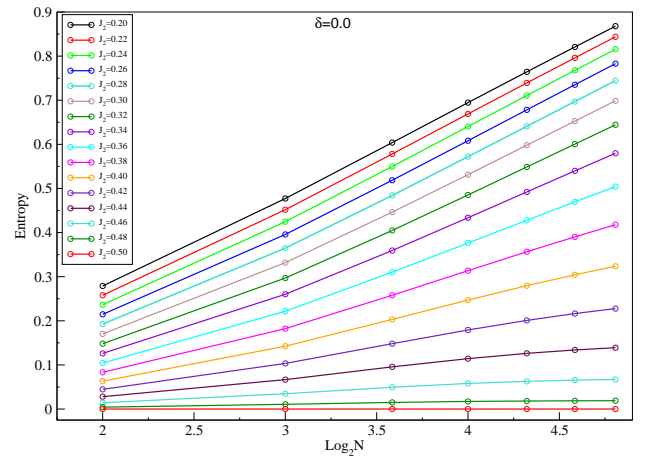


FIG. 4. For a spin-1/2 system, the entropy versus logarithm of the system size is shown for different J_2 values for a uniform chain.

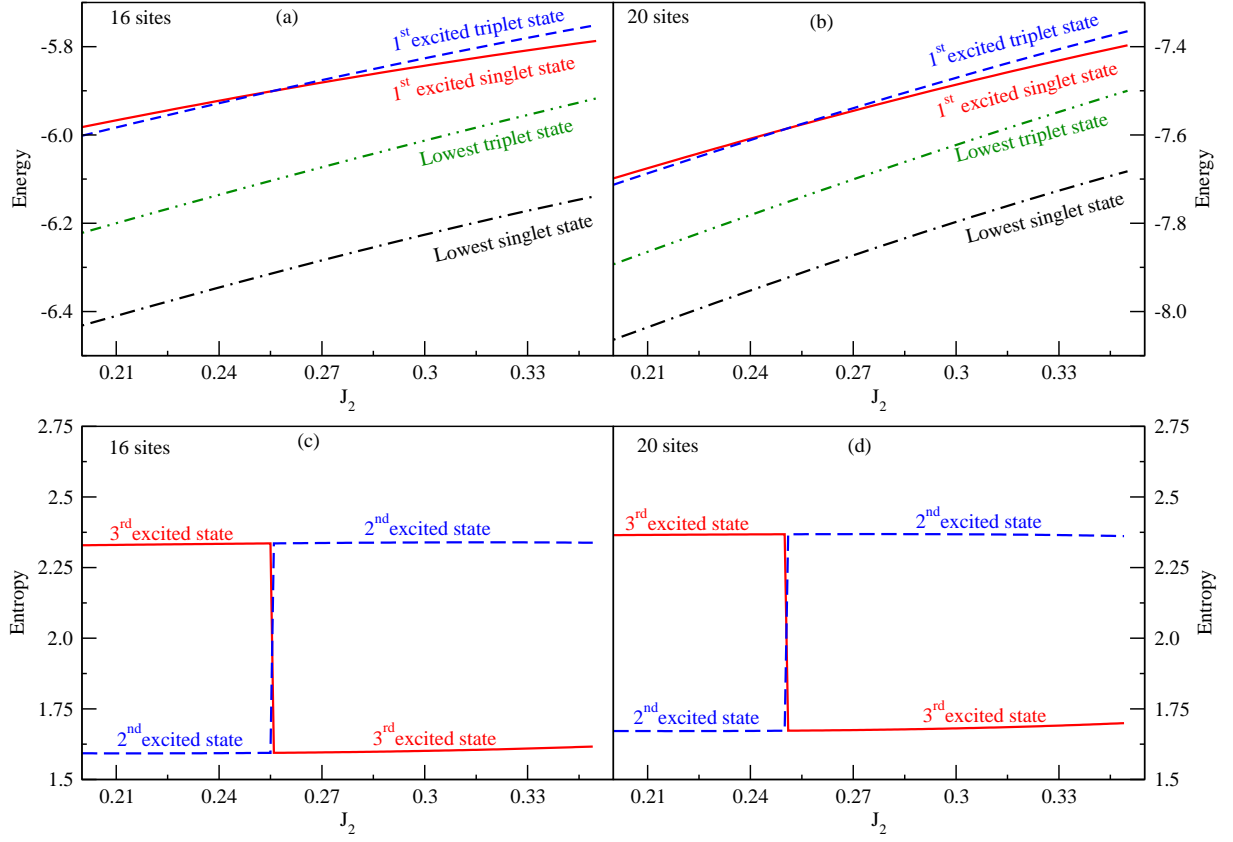


FIG. 5. Lowest and first excited state energies of the 16 and 20 sites spin-1/2 chain for different J_2 values with total spin $S=0$ and 1 are shown in (a) and (b). Entropy of the second excited state (dashed line) and third excited state (solid line) of 16 and 20 sites for different J_2 values in the $M_s = 0$ sector are shown in (c) and (d).

and their relative weights in a state under study, we can qualitatively understand the entropy of the state⁴⁴. In generating the contour plot of entropy, we have calculated the entropy over a grid of 201 J_2 values ($0 \leq J_2 \leq 2$) and 101 δ values ($0 \leq \delta \leq 1$).

V. RESULTS AND DISCUSSION

In this section, we present numerical results for the entanglement entropy of finite size chains with two equal block sizes for the spin-1/2, 1 and 3/2. We also present results for the ground state fidelity of both the systems in the $J_2 - \delta$ plane.

A. The spin-1/2 system in $J_2 - \delta$ plane

1. Uniform chain ($\delta = 0$)

The uniform spin-1/2 chain without dimerization ($\delta = 0$) goes through a gapless to gapped phase transition at $J_{2c} \simeq 0.2411$ in the thermodynamic limit ($N \rightarrow \infty$)⁴¹, and its Neel phase is separated from the spiral phase at

$J_2 = 0.5$. To study the behavior of the system around those points, we calculate the ground state fidelity and entanglement entropy of the system.

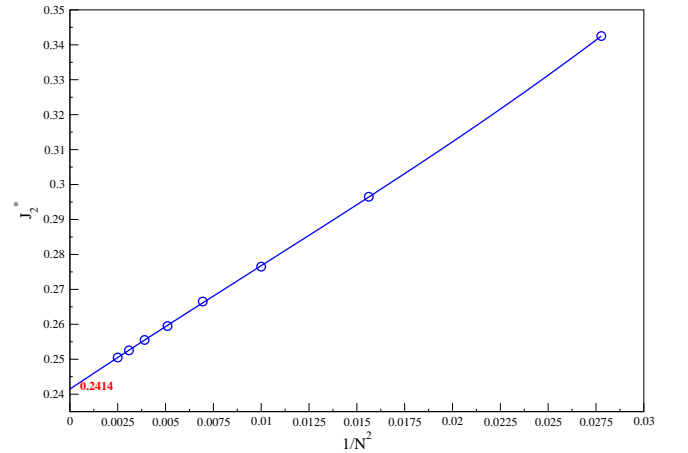


FIG. 6. Convergence of the crossing points of the excited states for a spin-1/2 chain.

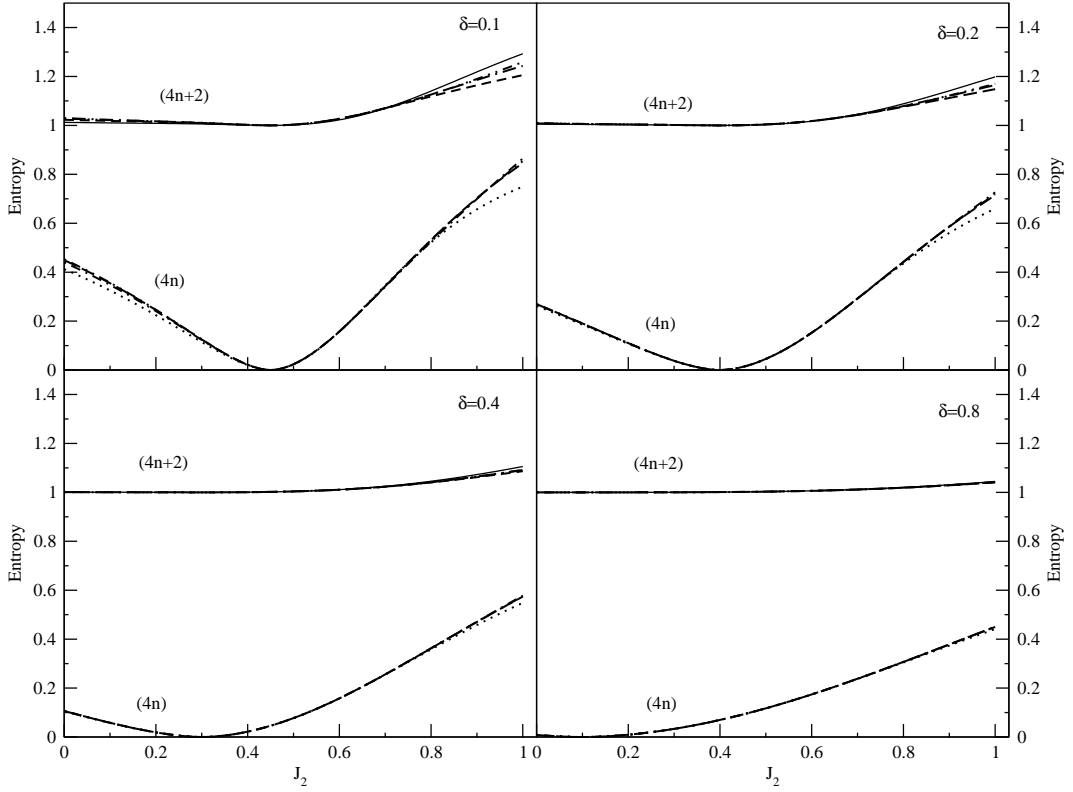


FIG. 7. Ground state entanglement entropy of a spin-1/2 chain with lengths of 6, 8, 10, 12, 14, 16, 18 and 20, for different values of δ values; the line types for different lengths are the same as in Fig. 3. The upper set of curves is for chain length $4n + 2$ while the lower one is for chain length $4n$ (n being a positive integer). Near the minimum, the finite size dependence is very weak.

trophy of finite size spin-1/2 chains with different J_2 values. The bipartite entropy for different chain lengths (and equal block size) can be seen in Fig. 3. At $J_2 = 0.5$, the entropy reaches a minimum; away from that point the entropy increases. For the systems with even block sizes, the minimum of the entropy goes to zero while for odd block sizes, this minimum is one. This result can be explained by noting that, at $J_2 = 0.5$ (the Majumdar-Ghosh point³⁴), the ground state has Kekule state structure (as in Fig. 2 (a)). Depending upon the block size being odd or even, entropy will be finite or zero respectively⁴⁴. As J_2 moves away from that point, the presence of other VB basis states (as in Fig. 2(b)) in the ground state will become significant. Since these VB basis states will have a finite entropy contribution, the entropy of the ground state will increase as J_2 moves away from the point.

We do not observe any change in the behavior of the ground state entropy around J_{2c} . To investigate this further, we plot the entropy versus $\log_2 N$ for different J_2 values (see Fig. 4). The plots indicate that the present system sizes are too small to numerically verify the conformal field theory prediction of $S = \frac{c}{6} \log_2 N$ (with $c = 1$) at J_{2c} ¹⁰. The first excited states in the singlet and triplet sectors cross as a function of J_2 . We have

calculated the entropy of these two states as a function of J_2 . We find that the entropy of a state depends only on its spin and not on its energy. Therefore as a function of energy level ordering the entropy shows a jump at a value of J_2^* which depends on the chain length. The jump in the value of the entropy can be seen from Fig. 5. In Figs. 5 (a) and (b), we see that the ground state (lowest singlet) and lowest triplet state are non-degenerate for finite N ; they become degenerate in the thermodynamic limit^{36,41}. However, the first excited singlet and the first excited triplet states become degenerate near J_{2c} even for small values of N . In Fig. 6 we plot the $J_2^*(N)$ as a function of $1/N^2$ and we see that J_2^* extrapolates to J_{2c} in the thermodynamic limit. The extrapolated value of J_2^* (0.2414) is very close to the reported value of $J_{2c} = 0.2411$ ^{36,41}.

Upon calculating the ground state fidelity (taking J_2 to be the variable parameter), we do not observe any behavioral change at $J_2 = 0.5$ or J_{2c} . The fidelity of first excited states in both the singlet and the triplet sectors falls to zero near J_{2c} . The same thing has already been observed for the system with periodic boundary conditions³¹.

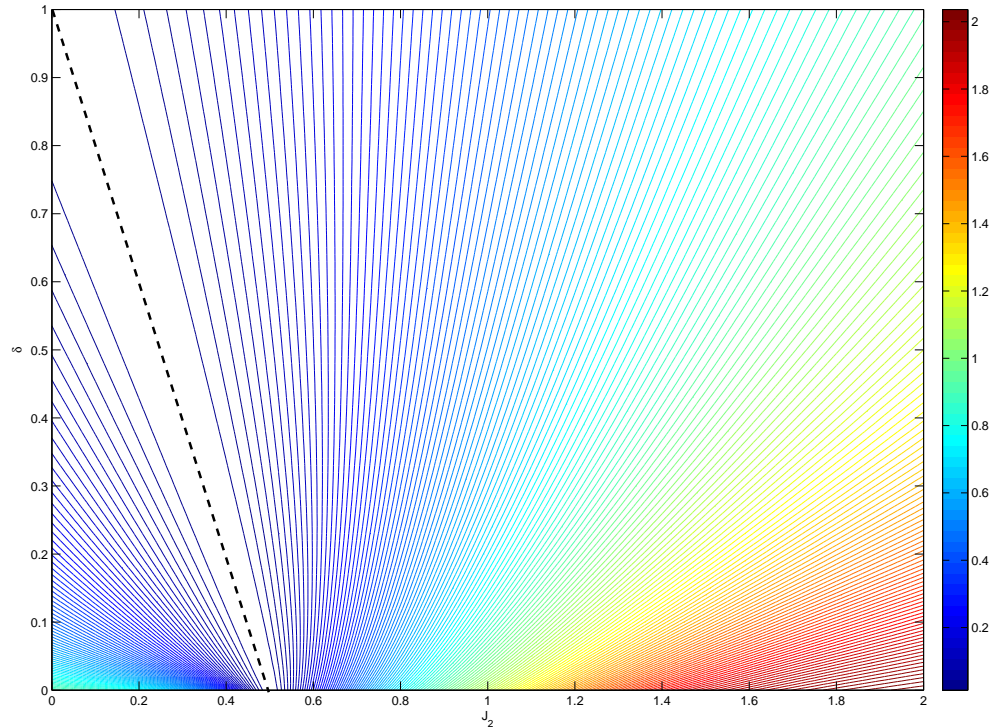


FIG. 8. Ground state entanglement entropy contour plot of spin-1/2 chain with 20 sites, for J_2 going from 0 to 2 and δ going from 0 to 1.

2. Dimerized chain ($0 < \delta \leq 1$)

In the phase diagram of the spin-1/2 system with dimerization, the Neel phase is separated from the spiral phase by the line $2J_2 + \delta = 1$. We study the ground state entanglement entropy of finite size chains in these phases with different δ values (see Fig. 7). We observe that the entropy of the system is minimum for values of J_2 and δ which fall on this line. For systems with even sized blocks, this minimum value is zero while for odd sized blocks the minimum is one. The reason for this is similar to the case $\delta = 0$ as given earlier.

We have calculated the ground state fidelity (with J_2 as the variable parameter) of finite size systems in the $J_2 - \delta$ plane; we do not observe any sudden change in fidelity along the $2J_2 + \delta = 1$ line. This can be explained by the fact that the phases of the system on both sides of the line are gapped which implies that the ground state does not cross any excited state (i.e., the ground state does not change its character of being a singlet or a triplet) when we cross this line in the parameter space.

3. Spin-1/2 entropy phase diagram (contour plot)

We study the gapless to gapped phase transition and change in the spin structure (order-disorder change) along the $2J_2 + \delta = 1$ line using the entropy contour plot for a spin-1/2 chain with 20 sites (see Fig. 8). The entropy is zero along this line. The density of the entropy contour lines shows whether the system is in a gapless or gapped phase. From this figure we see that the gapless region between $J_2 = 0$ and J_{2c} has a higher density of entropy contour lines. In the rest of the figure the density of the contour lines is lower which shows that the rest of the phase diagram is gapped. At higher values of J_2 , the spin-1/2 chain behaves like two decoupled chains with a weak coupling (J_1) between them. The stronger interaction (J_2) is responsible for the higher entropy. For higher values of both J_2 and δ values, the spin-1/2 chain behaves like a spin ladder with a gapped phase.

B. The spin-1 system in $J_2 - \delta$ plane

As mentioned in section III, there are many phases in the $J_2 - \delta$ phase diagram of the spin-1 system. To study these phases, we first calculate the bipartite entangle-

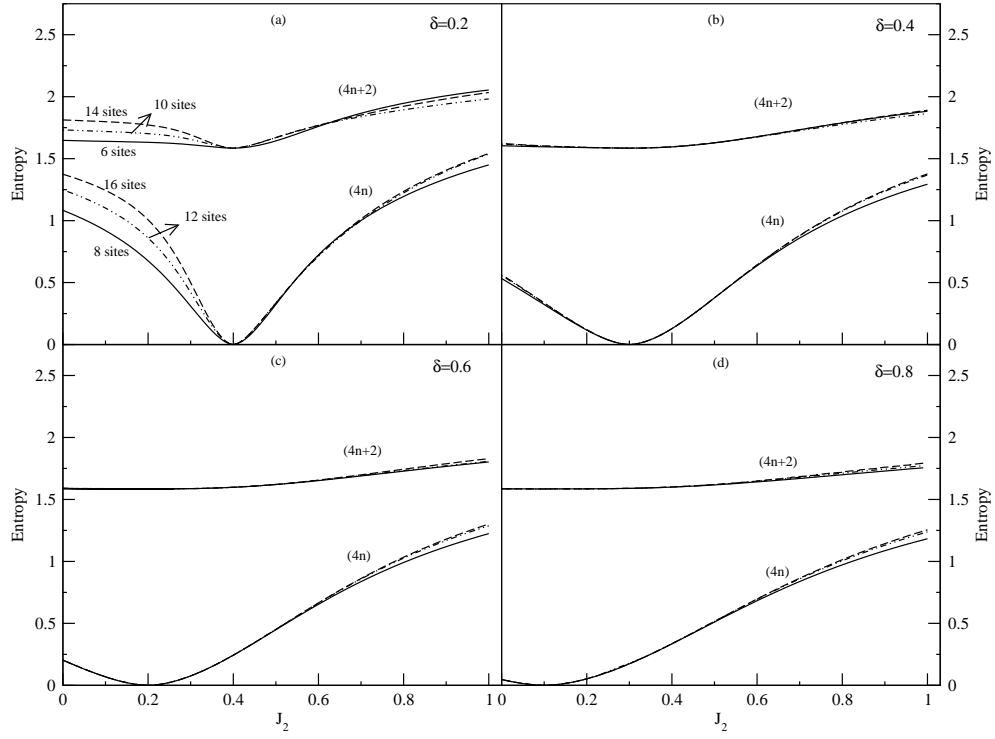


FIG. 9. Ground state entropy of the spin-1 system with different chain lengths and δ values along the J_2 axis. The line types for different chain lengths are the same as in (a).

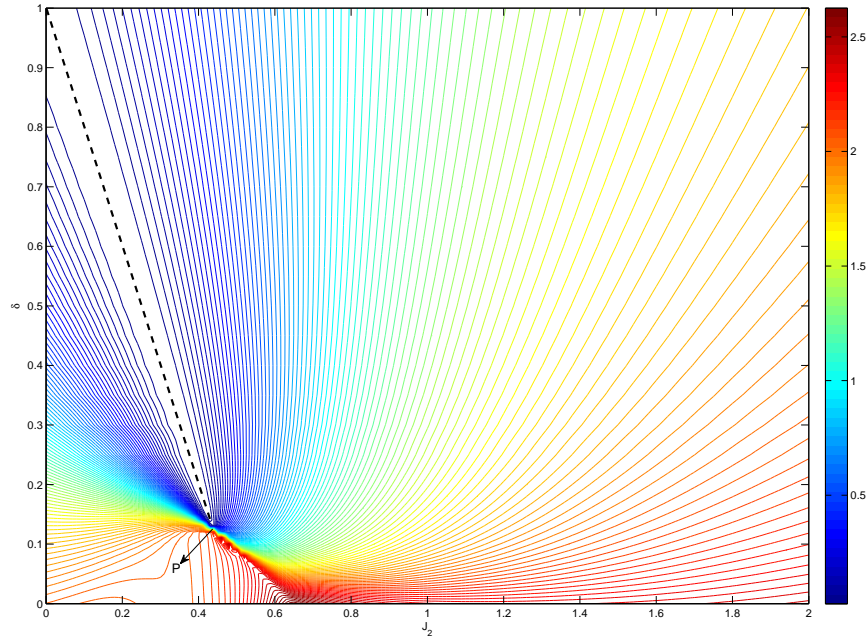


FIG. 10. Ground state entanglement entropy contour plot of a spin-1 chain with 16 sites, with J_2 going from 0 to 2 and δ going from 0 to 1.

ment entropy in the ground state for finite systems. We calculate the ground state entropy for different values of δ (with large δ) and for different chain lengths (see Fig. 9). The entropy is zero along the line $2J_2 + \delta = 1$ for the systems with even sized blocks and non-zero for systems with odd sized blocks just as in the spin-1/2 case. As in the spin-1/2 case, the finite size effects are very weak near the minima of the entropy (Fig. 9).

1. Spin-1 entropy phase diagram (contour plot)

In Fig. 1 (b), we know that the ground state is four-fold degenerate in regions II and III for an open chain. Hence we used the spin parity symmetry to break the degeneracy between the states corresponding to the total spin $S = 0$ and 1. Then we calculate the entanglement entropy for the lowest state in the even parity subspace (which is a singlet). We study the quantum phases and QPTs of the spin-1 chain with 16 sites using the contour plot of the ground state entropy in the $J_2 - \delta$ plane, where J_2 goes from 0 to 2 and δ goes from 0 to 1 (see Fig. 10). We see in the figure that the line $2J_2 + \delta = 1$ starts approximately at the point $P = (0.432, 0.136)$ and extends up to $(0, 1)$. Along this line the entropy is zero. Along the gapless lines ‘a’ and ‘c’ (in Fig. 1 (b)) the density of the entropy contour lines is higher, while the density is lower in the rest of the phase diagram. About the line ‘d’ (in Fig. 1 (b)), we observe that the density of contour lines is much lower compared to the regions near by.

In curve (i) of Fig. 11, we plot δ_{cal} versus J_2 for the

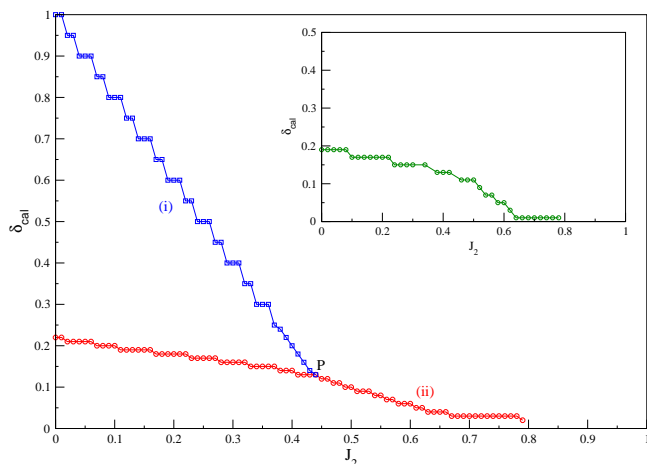


FIG. 11. Curve (i) shows the (J_2, δ_{cal}) values (squares) corresponding to the minimum entropy. Curve (ii) shows the (J_2, δ_{cal}) values (circles) corresponding to the maximum absolute values of the first order derivative of the entropy w.r.t. δ . Inset shows the points corresponding to minimum fidelity (taking δ as the variable parameter). All the results are obtained for the 16 site spin-1 chain.

trophy in the $J_2 - \delta$ plane; this curve goes from the point ‘P’ to the point $(0, 1)$. This curve is seen to follow the line $2J_2 + \delta = 1$ as expected; we see a step staircase instead of a straight line because we have calculated the entropy for discrete values of J_2 and δ . To detect the gapless phase along the lines ‘a’ and ‘c’, we calculate the first order derivative of the entropy (using the three-point differentiation formula) along the δ -axis for different values of J_2 in this plane. In curve (ii) of Fig. 11, we plot δ_{cal} versus J_2 corresponding to the maximum of the absolute value of the derivative. This curve follows the lines ‘a’ and ‘c’ closely.

2. Spin-1 chain fidelity and gap

We calculate the ground state fidelity of spin-1 chains with finite sizes in the $J_2 - \delta$ plane. For small values of δ , the ground states of finite size systems have multiple energy level crossings with the excited states. Because of these finite size effects, the fidelity of the ground states is not a reliable tool for studying phases in regions II and III. However in the regions I and IV, we find no energy level crossings in the ground states of finite systems. We calculate the ground state fidelity for systems with 6, 8, 10, 12 and 16 sites for different values of δ along the J_2 axis in this plane. We find no sudden changes in the fidelity. We show the plot of J_2 versus δ_{cal} corresponding to the minimum fidelity for a chain of 16 sites (see inset of Fig. 11). This curve follows the lines ‘a’, ‘b’, ‘ \bar{b} ’ and ‘c’ qualitatively separating regions II and III from regions I and IV.

To understand the quantum phase transition on the line ‘b’ in Fig. 1, we calculate the spin gap of the system near this line (see Fig. 12). Since the ground state of an open chain with spin-1 is four-fold degenerate in the regions II and III, we calculate the excitation energy gap as the difference between the lowest energy state in the $M_s = 0$ sector and the first excited state in the $M_s = 1$ sector. Our current calculations based on a finite size analysis shows that the gap could vanish in the thermodynamic limit. This improves our earlier report which had convergence difficulties^{38,39}. We also studied the behavior of the gap across the lines ‘b’ and ‘ \bar{b} ’. For example, for the 16 site chain, the gap is minimum at $\delta \simeq 0.13$ at $J_2 = 0.4$ and $\delta \simeq 0.09$ at $J_2 = 0.5$ (see insets of Fig. 12). Also there is a change in the behavior of the gap versus $1/N$ as δ varies; for δ lying below the phase transition line, the gap saturates to a finite value, while for δ lying above the line, the gap continues to decrease steadily as N increases.

The line ‘b’ appears to be a phase transition line which separates the Haldane and spin Peierls phases which are both gapped. These two phases differ in several ways. For an open chain, the ground state has a four-fold degeneracy (a spin singlet and a spin triplet which are degenerate) with spin-1/2 states at the ends in the Haldane phase, but is non-degenerate (spin singlet) in the

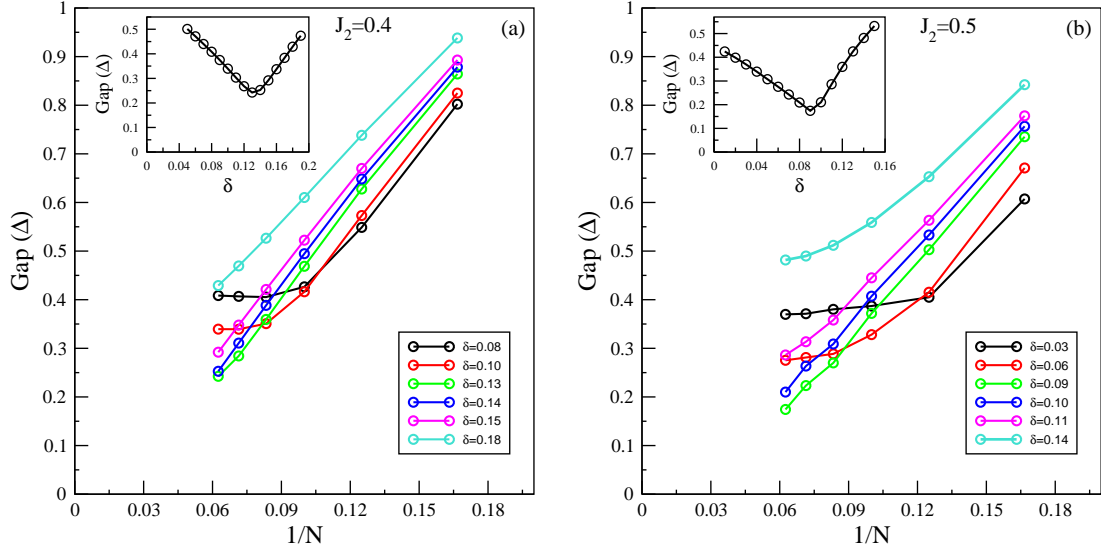


FIG. 12. Figures show how a plot of the gap (Δ) versus $1/N$ changes with δ for (a) $J_2=0.4$ and (b) $J_2=0.5$ which lie on the dotted lines ‘b’ and ‘b’ respectively in Fig. 1(b). Here the gap represents $\Delta = E_1(M_s = 1) - E_0(M_s = 0)$. Insets show how the gap varies with δ for the 16 site spin-1 chain. See section V.B.2 for details.

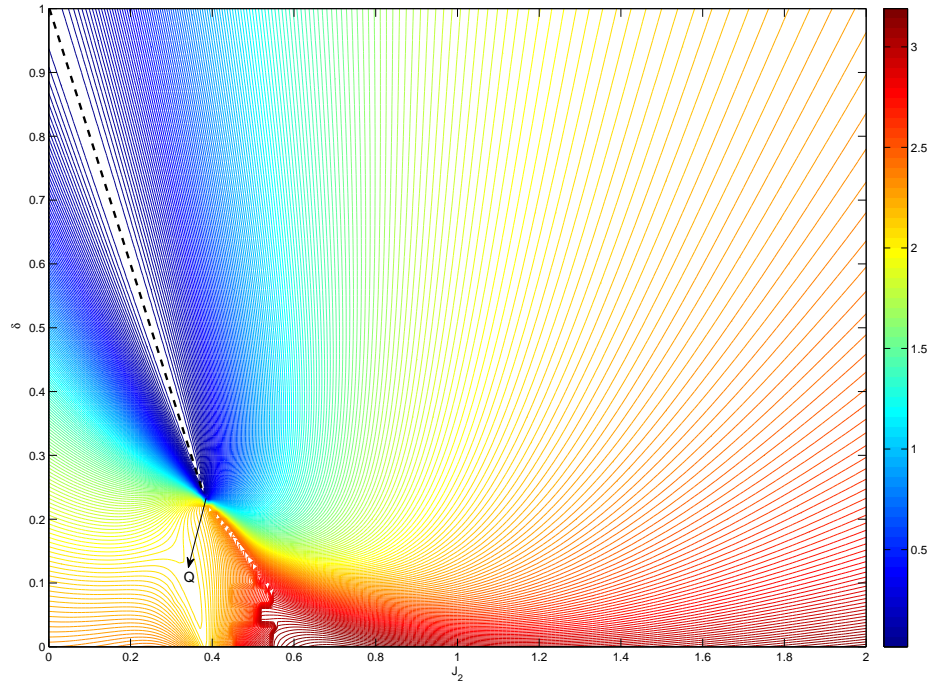


FIG. 13. Ground state entanglement entropy contour plot of a spin-3/2 chain with 12 sites, with J_2 going from 0 to 2 and δ going from 0 to 1.

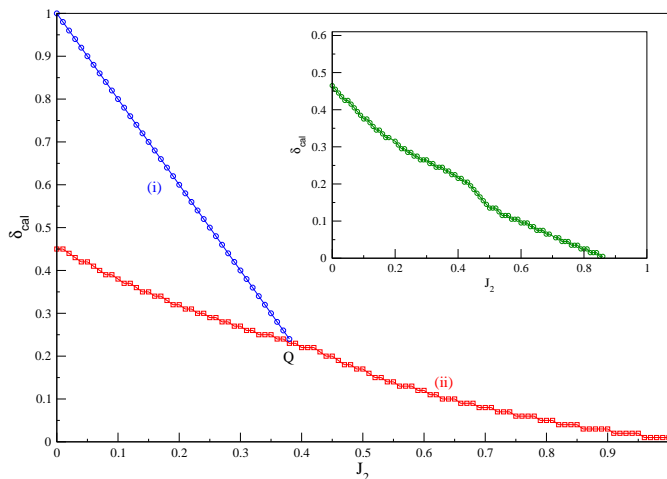


FIG. 14. Curve (i) shows the (J_2, δ_{cal}) values (squares) corresponding to the minimum entropy. Curve (ii) shows the (J_2, δ_{cal}) values corresponding to the maximum absolute values of the first order derivative of the entropy w.r.t. δ . Inset shows the points corresponding to minimum fidelity (taking δ as the variable parameter). All the results are obtained for the 12 site spin-3/2 chain.

spin Peierls phase. Further, the Haldane phase has a non-local string order parameter⁴⁸.

C. The spin-3/2 system in $J_2 - \delta$ plane

In this section we study the phase diagram of the spin-3/2 system in the $J_2 - \delta$ plane. To the best of our knowledge, the quantum phases of the Heisenberg spin-3/2 antiferromagnetic chain in the $J_2 - \delta$ plane has not been studied earlier. But from the field theory analysis of the spin chain, half-odd integer systems are gapless at $\delta = 0$ and for small values of J_2 . With dimerization ($\delta \neq 0$), it is predicted that spin-3/2 system should be gapless at $\delta = 2/3$ for $J_2 = 0$ ^{39,49}.

1. Spin-3/2 entropy phase diagram (contour plot)

We study different quantum phases of spin-3/2 chain. We use spin parity symmetry to break the degeneracy (within numerical accuracy) of the ground state of this system. For 12 site chain, a contour plot of the entropy is shown in Fig. 13. As in the spin-1/2 and spin-1 cases, we observe an order-disorder transition along $2J_2 + \delta = 1$ line. The line starts approximately from the point Q = $(J_2 = 0.38, \delta = 0.24)$ and extends up to $(J_2 = 0, \delta = 1)$. For small J_2 values near $\delta = 0$ in the contour plot, the line pattern is similar to that for spin-1/2 case and quite different from the spin-1 case. This suggests that there can be a gapless phase at $\delta = 0$ as predicted. For $J_2 = 0$, the line density is very high between $\delta = 0.4$ and 0.5 ; this

suggests another gapless phase in this region as predicted by field theory. As in the spin-1 case, the density of lines is high at larger J_2 values (about $J_2 = 1$). This suggests a numerically gapless phase in this region. We also confirm these gapless phases by comparing numerical energy gaps in those regions with that of a phase at large values of J_2 and δ where the density of lines is very low. For better understanding of these quantum phases we plot δ_{cal} versus J_2 values corresponding to the minimum entropy (curve (i) from Fig. 14) above the ‘Q’ point. This curve follows the $2J_2 + \delta = 1$ line similar to the spin-1/2 and spin-1 cases. We also plot the points corresponding to the maximum absolute values of the first order derivative of entropy with respect to δ ; this is shown as curve (ii) in Fig. 14. This is similar to the curve representing a numerically gapless phase for a spin-1 system (curve (ii) in Fig. 11). This suggests that there can also be a gapless region along the curve (ii) for spin-3/2 system. The gapless point (curve (ii) of Fig. 14) at $\delta = 0.45$ at $J_2 = 0$ is consistent with the value $\delta = 0.431$ reported⁵⁰. Note that this value is different from the field theory prediction of $2/3$ ^{39,49}.

We calculate the ground state fidelity of the 12 site spin-3/2 chain along different J_2 values with δ as the variable parameter. We plot J_2 versus δ correspond to minimum fidelity in this plane (see inset of Fig. 14). The curve approximately follows the curve (ii) in Fig. 14.

To further investigate the gapless points which are expected to occur at certain non-zero values of δ at $J_2 = 0$ for the spin-1 and 3/2 systems, we have shown the entropy versus the logarithm of the system size for different δ values in Fig. 15. The present system size appears to be too small to numerically verify the conformal field theory prediction¹⁰ of $S = \frac{c}{6} \log_2 N$ (with $c = 1$) at the critical points which occur at certain values of δ (numerically estimated to be 0.24 for spin-1 and 0.43 for spin-3/2).

VI. CONCLUSION

We have used entanglement entropy and fidelity as tools to study the different quantum phases and quantum critical regions of the spin-1/2, 1 and 3/2 chains in the $J_2 - \delta$ plane. For this study, we have employed extensive exact diagonalization of spin chains with up to 20 sites depending on the site spin. We have considered 201 values of J_2 in the range 0 to 2 and 101 values of δ in the range 0 to 1 corresponding to over 20,000 grid points.

We have studied the complete phase diagrams of these three systems using entropy contour plots and fidelity in the $J_2 - \delta$ plane. We have been able to identify the quantum phase transitions from gapless to gapped phases using the density of the contour lines of the entropy and the minimum fidelity. Though the full phase diagram of the spin-3/2 system has not been investigated before, we have conjectured the existence of some gapless regions and an order-disorder line by studying its phase diagram and comparing it with the phase diagrams of the spin-

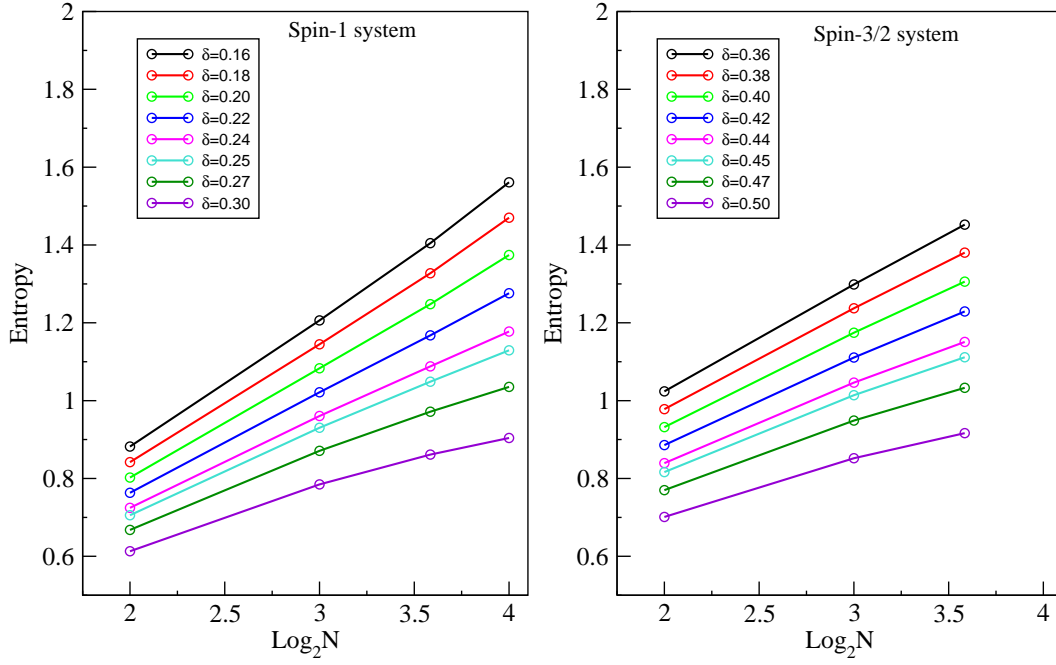


FIG. 15. For spin-1 and 3/2 systems, the entropy versus logarithm of the system size is shown for different δ values with $J_2 = 0$.

1/2 and spin-1 systems. Our main results are that we find indications of a gapless region near $\delta = 0$ and small values of J_2 in the spin-1/2 system, a gapless region at finite δ in the spin-1 system (lines ‘a’ and ‘b’ in Fig. 1 (b)), and two gapless regions near $\delta = 0$ and around

$\delta \sim 0.4 - 0.5$ for $J_2 = 0$ in the spin-3/2 system.

VII. ACKNOWLEDGMENT

S. R. and D. S. are thankful to the Department of Science and Technology (DST), India for financial support through various projects.

* gvmldurgaprasad@sscu.iisc.ernet.in

† shaon@physics.iisc.ernet.in

‡ ramasesh@sscu.iisc.ernet.in

§ diptiman@cts.iisc.ernet.in

¹ R. Horodecki, P. Horodecki, M. Horodecki and K. Horodecki, Rev. Mod. Phys. **81**, 865 (2009).

² L. Amico, R. Fazio, A. Osterloh and V. Vedral, Rev. Mod. Phys. **80**, 517 (2008).

³ S. Sachdev, Nature Physics **4**, 173 (2008).

⁴ G. Vidal, J. I. Latorre, E. Rico and A. Kitaev, Phys. Rev. Lett. **90**, 227902 (2003); J. I. Latorre, E. Rico and G. Vidal, Quant. Inf. Comput. **4**, 48 (2004).

⁵ B. Jin and V. E. Korepin, J. Stat. Phys. **116**, 79 (2004); A. R. Its, B. -Q. Jin and V. E. Korepin, J. Phys. A **38**, 2975 (2005).

⁶ G. Refael and J. E. Moore, Phys. Rev. Lett. **93**, 260602 (2004), and J. Phys. A **42**, 504010 (2009).

⁷ D. Larsson and J. Henrik, Phys. Rev. Lett. **95**, 196406 (2005).

⁸ T. Barthel, S. Dusuel and J. Vidal, Phys. Rev. Lett. **97**, 220402 (2006).

⁹ N. Laflorencie, E. S. Sørensen, M.-S. Chang and I. Affleck, Phys. Rev. Lett. **96**, 100603 (2006).

¹⁰ P. Calabrese and J. Cardy, J. Phys. A **42**, 504005 (2009).

¹¹ L. Tagliacozzo, T. R. de Oliveira, S. Iblisdir and J. I. Latorre, Phys. Rev. B **78**, 024410 (2008).

¹² F. Pollmann, S. Mukerjee, A. M. Turner and J. E. Moore, Phys. Rev. Lett. **102**, 255701 (2009).

¹³ J. I. Latorre and A. Riera, J. Phys. A **42**, 504002 (2009).

¹⁴ M. Znidaric and T. Prosen, J. Phys. A **36**, 2463 (2003).

¹⁵ P. Zanardi and N. Paunkovic, Phys. Rev. E **74**, 031123 (2006).

¹⁶ L. Campos Venuti and P. Zanardi, Phys. Rev. Lett. **99**, 095701 (2007).

¹⁷ P. Zanardi, P. Giorda and M. Cozzini, Phys. Rev. Lett. **99**, 100603 (2007).

¹⁸ P. Buonsante and A. Vezzani, Phys. Rev. Lett. **98**, 110601 (2007).

¹⁹ W.-L. You, Y.-W. Li and S.-J. Gu, Phys. Rev. E **76**, 022101 (2007); S.-J. Gu, H.-M. Kwok, W.-Q. Ning and H.-Q. Lin, Phys. Rev. B **77**, 245109 (2008); S.-J. Gu and H.-Q. Lin, EPL **87**, 10003 (2009); S.-J. Gu, Int. J. Mod. Phys B **24**, 4371 (2010); S. Yang, S.-L. Gu, C.-P. Sun and H.-Q. Lin,

- Phys. Rev. A **78**, 012304 (2008).
- ²⁰ J. Ma, L. Xu, H.-N. Xiong and X. Wang, Phys. Rev. E **78**, 051126 (2008).
 - ²¹ H.-Q. Zhou, R. Orus and G. Vidal, Phys. Rev. Lett. **100**, 080601 (2008); H.-Q. Zhou, J. H. Zhao and B. Li, J. Phys. A **41**, 492002 (2008); H.-Q. Zhou and J. P. Barjaktarevic, J. Phys. A, **41** 412001 (2008); J.-H. Zhao and H.-Q. Zhou, Phys. Rev. B **80**, 014403 (2009).
 - ²² D. Schwandt, F. Alet and S. Capponi, Phys. Rev. Lett. **103**, 170501 (2009); A. F. Albuquerque, F. Alet, C. Sire and S. Capponi, Phys. Rev. B **81**, 064418 (2010).
 - ²³ E. Eriksson and H. Johannesson, Phys. Rev. A **79**, 060301(R) (2009).
 - ²⁴ V. Gritsev and A. Polkovnikov, arXiv:0910.3692 (2009), published in *Understanding Quantum Phase Transitions*, edited by L. D. Carr (Taylor and Francis, Boca Raton, 2010); C. De Grandi, V. Gritsev, and A. Polkovnikov, Phys. Rev. B **81**, 012303 (2010); C. De Grandi, V. Gritsev and A. Polkovnikov, Phys. Rev. B **81**, 224301 (2010).
 - ²⁵ A. Polkovnikov, K. Sengupta, A. Silva and M. Vengalattore, Rev. Mod. Phys. **83**, 863 (2010).
 - ²⁶ J. Sirker, Phys. Rev. Lett. **105**, 117203 (2010).
 - ²⁷ M. M. Rams and B. Damski, Phys. Rev. Lett. **106**, 055701 (2011); M. M. Rams and B. Damski, Phys. Rev. A **84** 032324 (2011).
 - ²⁸ V. Mukherjee, A. Polkovnikov and A. Dutta, Phys. Rev. B **83**, 075118 (2011); V. Mukherjee and A. Dutta, Phys. Rev. B **83**, 214302 (2011); V. Mukherjee, A. Dutta and D. Sen, Phys. Rev. B **85**, 024301 (2012).
 - ²⁹ F. Alet, I. P. McCulloch, S. Capponi and M. Mambrini, Phys. Rev. B **82**, 094452 (2010).
 - ³⁰ R. W. Chhajlany, P. Tomczak, A. Wójcik and J. Richter, Phys. Rev. A **75**, 032340 (2007).
 - ³¹ S. Chen, L. Wang, S.-J. Gu and Y. Wang, Phys. Rev. E **76**, 061108 (2007).
 - ³² M. Thesberg and E. S. Sørensen, Phys. Rev. B **84**, 224435 (2011).
 - ³³ L. Campos Venuti, C. Degli Esposti Boschi and M. Roncaglia, Phys. Rev. Lett. **96**, 247206 (2006).
 - ³⁴ C. K. Majumdar and D. K. Ghosh, J. Math. Phys. **10**, 1388 (1969).
 - ³⁵ S. R. White, Phys. Rev. Lett. **69**, 2863 (1992), and Phys. Rev. B **48**, 10345 (1993).
 - ³⁶ R. Chitra, S. Pati, H. R. Krishnamurthy, D. Sen and S. Ramasesha, Phys. Rev. B **52**, 6581 (1995).
 - ³⁷ K. Totsuka, Y. Nishiyama, N. Hatano and M. Suzuki, J. Phys. Condens. Matter **7**, 4895 (1995); Y. Kato and A. Tanaka, J. Phys. Soc. Jpn. **63**, 1277 (1994).
 - ³⁸ S. Pati, R. Chitra, D. Sen, H. R. Krishnamurthy and S. Ramasesha, Europhys. Lett. **33**, 707 (1996).
 - ³⁹ S. Pati, R. Chitra, D. Sen, S. Ramasesha and H. R. Krishnamurthy, J. Phys. Condens. Matter **9**, 219 (1997).
 - ⁴⁰ S. R. White and I. Affleck, Phys. Rev. B **54**, 9862 (1996).
 - ⁴¹ K. Okamoto and K. Nomura, Phys. Lett. A **169**, 433 (1992).
 - ⁴² J. Almeida, M. A. Martin-Delgado and G. Sierra, AIP Conf. Proc. **918**, 261 (2007).
 - ⁴³ S. K. Pati, S. Ramasesha and D. Sen, in *Magnetism: Molecules to Materials IV*, edited by J. S. Miller and M. Drillon (Wiley-VCH, 2002), chap. 4.
 - ⁴⁴ S. Sahoo, V. M. L. Durga Prasad Goli, S. Ramasesha and D. Sen, J. Phys.: Condens. Matter **24**, 115601 (2012).
 - ⁴⁵ L. Pauling, J. Chem. Phys. **1**, 280 (1933); L. Pauling and G. W. Wheland, *ibid*, **1**, 362 (1933).
 - ⁴⁶ Z. G. Soos and S. Ramasesha, in *Valence Bond Theory and Chemical Structure*, edited by D. J. Klein and N. Trinajstić (Elsevier, New York, 1990), p. 81; S. Ramasesha and Z. G. Soos, in *Valence Bond Theory*, edited by D. L. Cooper (Elsevier, New York, 2002), chap. 20.
 - ⁴⁷ S. Sahoo, R. Rajamani, S. Ramasesha and D. Sen, Phys. Rev. B **78**, 054408 (2008).
 - ⁴⁸ M. den Nijs and K. Rommelse, Phys. Rev. B **40**, 4709 (1989).
 - ⁴⁹ I. Affleck and F. D. M. Haldane, Phys. Rev. B **36**, 5291 (1987).
 - ⁵⁰ M. Nakamura and S. Todo, Phys. Rev. Lett. **89**, 077204 (2002).